Jordan Journal of Civil Engineering, Volume **19**, No. **1**, **2025**
DOI: https://doi.org/10.14525/JJCE.v19i1.09

Jordan Journal of Civil Engineering

Journal homepage: https://jjce.just.edu.jo

Dam Breach Risk Analysis and Mapping: A Case Study of the Wala Dam, Jordan

Radwan Al-Weshah [1), 2)*]***, Anwar Tarawneh*** [3)]***, Murad Al-Salahat*** [4)]

[1)] *Professor, Civil Engineering Department, The University of Jordan, Amman 11942, Jordan. E-Mail: r.weshah@ju.edu.jo*
[2)] *Professor, Department of Civil Engineering, Faculty of Engineering and Technology, Al-Zaytoonah University of Jordan, Amman 11733, Jordan. * Corresponding Author. E-Mail: r.weshah@zuj.edu.jo*
[3)] *Instructor, Department of Civil Engineering, Faculty of Engineering and Technology, Al-Zaytoonah University of Jordan, Amman 11733, Jordan. E-Mail: anwar.tarawneh@zuj.edu.jo*
[4)] *Project Coordinator Engineer, World Vision International, Amman 11855, Jordan. E-Mail: murad_alsalahat@wvi.org*

ARTICLE INFO

Article History:
Received: 3/10/2024
Accepted: 27/12/2024

ABSTRACT

This paper investigates the flood hazard related to dam breach analysis for Wala Dam in Jordan. Hydrologic modeling of probable maximum flood was conducted using the probable maximum precipitation values in the dam watershed. The peak probable maximum flood of the Wala dam watershed was about 2,621 m^3/s. Two dam breach scenarios were investigated; namely, overtopping and piping failures, using empirical dam breach equations. A 2-dimensional unsteady hydraulic model (HEC-RAS) was used to route the breach flood downstream of the dam. The maximum peak flows for both the overtopping and piping scenarios were 12,435 m^3/s and 5,962 m^3/s, respectively. The results are used to generate inundation, flood hazard risk, duration, and velocity maps for areas downstream of the dam. Most inundated areas were classified as extreme hazard areas. The maximum depth of water for overtopping failure is approximately 43 m in some agricultural lands and about 8 m near the Dead Sea road. Flooded areas include farmhouses, roads and bridges, the Dead Sea road and other important public and private properties. Furthermore, the maximum velocities are 17.1 m/s and 15.8 m/s for overtopping and piping failures, respectively. This study demonstrates the importance of developing and regularly updating comprehensive emergency preparedness and enhancing the resilience of downstream communities by community-based disaster risk reduction programs.

Keywords: Dam breach, Flood risk mapping, Wadi Wala dam, HEC-RAS modeling, Flood hydrology, Overtopping.

INTRODUCTION

Dam failure constitutes an uncontrollable catastrophe due to the immense energy unleashed by the accumulation and rapid flow of water in various scenarios (Guimarães et al., 2022). However, engineering factors can be predicted, including errors in overtopping due to poor spillway design, blockages, design flaws arising from unstable slopes, seepage penetrating through the structure and foundations, varying uplift pressures, and hydraulic changes within the dam structure, with the most recent being pipe failure (Alhasan et al., 2015; Latrubesse et al., 2020). Dam failure due to overtopping constitutes 90% of the total failure in the world (Zhang et al., 2021).

Overtopping failure happens when a dam is unable to adequately release the flowing water, resulting in difficulty controlling the volume of water retained

(Jiang et al., 2019). When water surpasses the designated level and other influencing factors come into play, this initiates the formation of a flood at the crest of the dam, leading to a breach caused by overtopping (Liu et al., 2023). The foremost challenge in dam safety revolves around devising effective solutions to assess risk and prevent the overtopping-induced failure of both new and existing dams. Hydrological safety stands as one of the most dynamic domains within dam engineering research, engaging a significant technical community globally (Caballero et al., 2022). Floods stemming from overtopping can arise from sudden and intense rainfall within a brief timeframe (Almawas et al., 2024). Alternatively, floods may also ensue from the failure of the dam due to various factors (Yilmaz et al., 2023). In the flood routing simulation for the overtopping failure of dams, the main risk factors can be divided into three primary groups: the stochastic nature of the inflow process to the reservoir, the unpredictable dam breach process, and the reliability flood routing process. The most important condition is partially dictated by the inflow hydrograph to the reservoir. Uncertainty in the inflow process originates from the unpredictable nature of natural inflows. Despite this inherent uncertainty hydrological analysis typically identifies the most severe flood scenario by considering statistical frequency analysis and extreme worst-case conditions. Consequently, the uncertainty in the inflow hydrograph of the reservoir can be excluded. Thus, uncertainty in dam breach flood analysis primarily stems from dam breach empirical simulation and the hydraulics of flood routing (Yang et al., 2023). Numerous instances of dam failure brought on by overtopping have been documented, such as the Teton Dam in Idaho and the Kelly Barnes Dam in near Toccoa (Yilmaz et al. 2023). In the failure of the Laurel dam in Johnston (Gray, 2017), 300 million m^3 of water leaked downstream in 1976 as a result of the Teton dam failure (Solava & Delatte, 2003). The two major factors in analyzing the failure of a dam focus on estimating the outflow hydrograph of the reservoir and the routing of flood wave downstream through the valley to assess the impact of the most probable dam failure (Beza et al., 2023). Accurately predicting the flood outflow hydrograph and its travel time after the failure process is very crucial in any emergency planning process, especially life of people being at risk downstream to the dam (Imbrogno, 2014). During the dam failure event, modeling becomes essential for assessing the flood waves stemming from the dam breach (Duressa & Jubir, 2018). Determining the area and depth of flooding was made easier by integrating a geographic information system (GIS) with the Hydrologic Engineering Centre-River Analysis System (HEC-RAS) simulation model. In particular, the 2D–3D HEC–RAS model was used to simulate the dam beach. Through precise assessment of flood hazards and the application of efficient flood management techniques, this can significantly reduce the risk of flooding (Vozinaki et al., 2017).

MATERIALS AND METHODS

Study Area

The Wala Dam (WD) is located at 31° 34' 5.04 " north and 35° 48' 16.5" east, nearly 40 km south of Amman city. The upstream watershed of WD has an area of 1,773.7 km^2, which extends to the east of the dam. This area forms the northern part of the Mujib basin drainage, which has an area of 6,600 km^2. The catchment area is drained through the Wala valley, descending from approximately 850 meters to 100 meters above mean sea level. Eventually, it converges with the Mujib valley before reaching the Dead Sea (Tarawneh, 2022). The dam was constructed as roller compacted concrete with a clay core. The height of the dam at the beginning of its construction was 42 meters above the foundation. Due to frequent flooding, the dam was raised to a new capacity of about 25 million cubic meters in 2022 (Salamah et al., 2023). Annual rainfall averages decline from over 300 mm at the western edge of the basin to less than 50 mm toward the eastern boundary (Farhan, 2017). The mean annual rainfall across the watershed ranges from 346 mm at Madaba, located several kilometers northwest of the watershed, to 282 mm at Dhiban and 266 mm at the Wadi Wala weather station. Notable seasonal temperature fluctuations are observed, with daily temperatures ranging from about 40˚C in August to a minimum of -5˚C in January. The annual potential evaporation rates vary from 1650 mm in the western highlands to more than 2100 mm in the eastern dry part of the catchment (Ta'any, 2011). Figure (1) shows the location of Wala dam in Jordan and Table 1 shows the general characteristics for Wala dam.

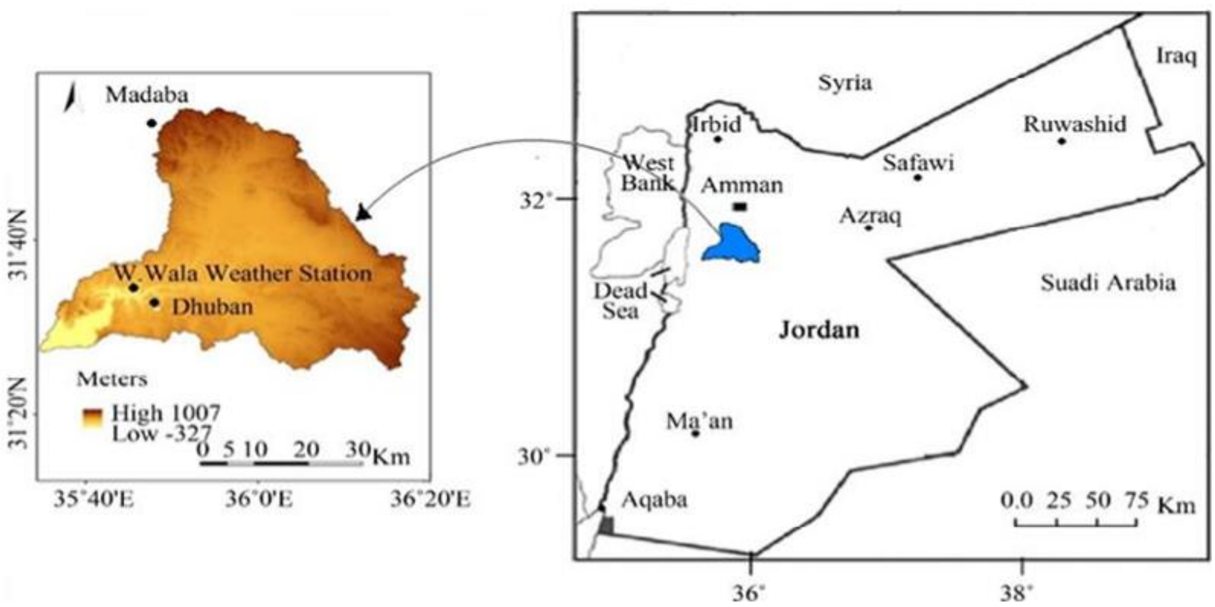

Figure (1): General location of the Wadi Wala watershed area (Farhan, 2017)

Table 1. General details for Wala dam in Jordan (Farhan, 2017)

Dam Parameter	RCC & Earth Fill
Length (m)	480
Crest width (m)	9
Height (m)	54
Catchment area (km^2)	1770
Storage at full supply level (MCM)	25

The watershed modeling system (WMS) is a rainfall-run-off model that simulates the process of converting precipitation into surface run-off in watersheds. This model aids in understanding precipitation events in streams. HEC-RAS, a hydrodynamic model, illustrates the spread and depth of flood inundation during rainfall over the watershed area, forming the basis for the flood map. Figure (2) shows the flow chart for the WMS and HEC-RAS modeling steps.

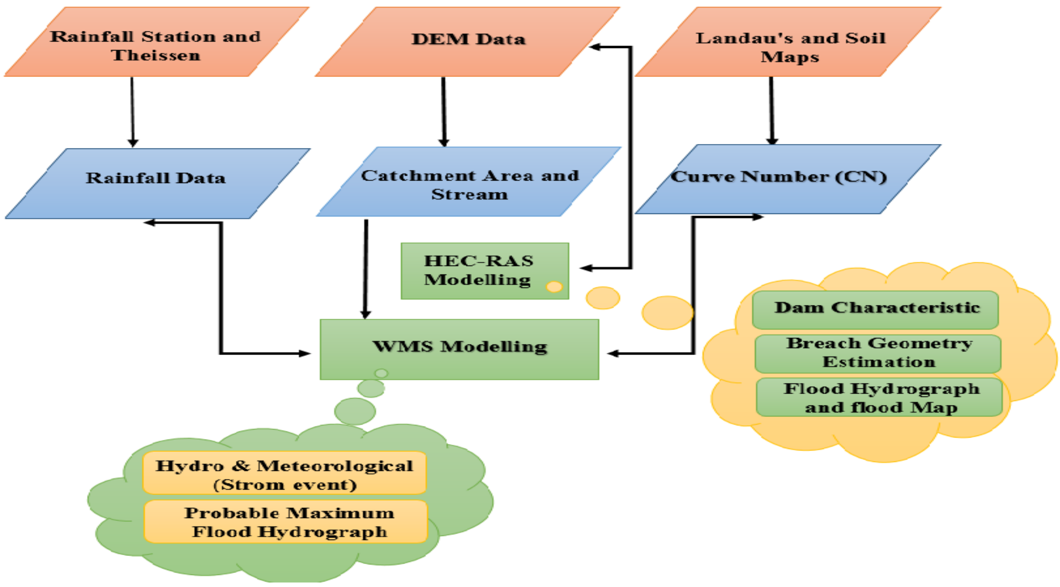

Figure (2): Schematic diagram for the WMS hydrology and HEC-RAS hydraulic modeling steps

Data Collection

Digital Elevation Model (DEM)

The digital elevation model (DEM) is a crucial input for hydraulic modeling, providing precise information about terrain elevation within the catchment area. Figure (3) displays the DEM for the Wala basin upstream of the Dam based on LiDAR or satellite imagery of 30-m resolution processed by WMS.

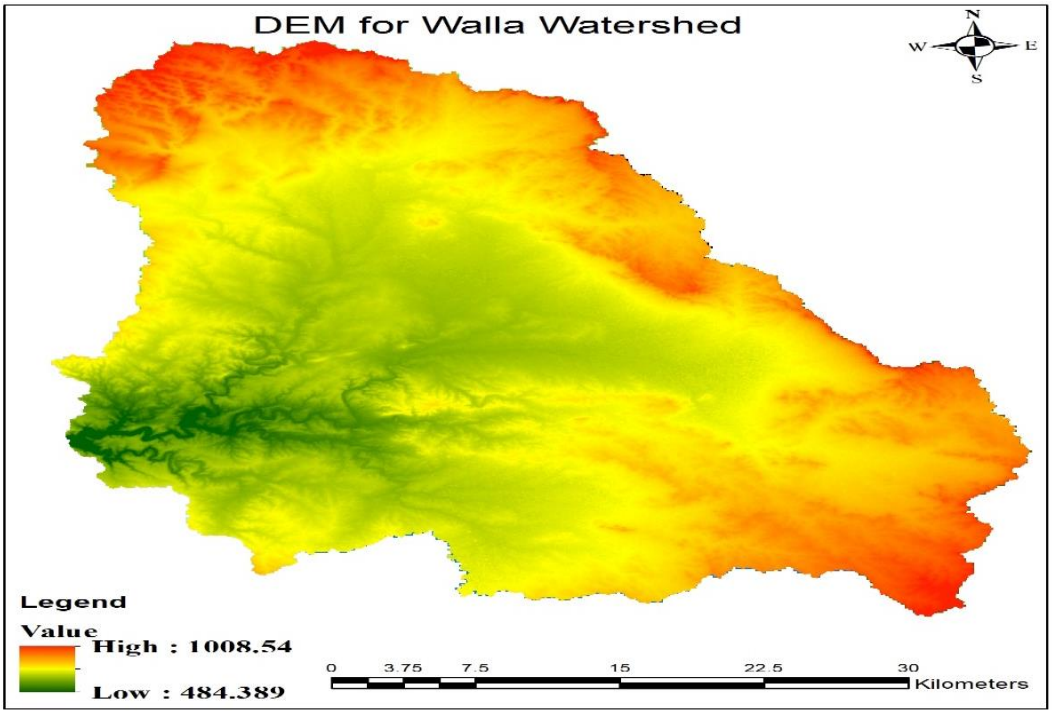

Figure (3): DEM of the study area (WMS, 2024)

Land Use/Cover (LULC)

The land use/cover map for the Wala basin was obtained as 10-meter resolution GeoTIFF files from the Esri 2022 Land cover map, produced by Impact Observatory. This map, derived from ESA Sentinel-2 imagery, is a composite of land use/land cover predictions for 10 classes throughout the year, generating a representative snapshot of 2020. To align land use with the LULC types and crop parameters for the Soil & Water Assessment Tool (SWAT) data, the land use map has undergone reclassification. A lookup table was prepared to identify the SWAT 10 land-use codes for the different LULC categories, relating the grid values to SWAT LULC classes.

In the Wala basin, barren areas, farmland, forests, rangelands, urban areas, and water bodies (reservoirs) are the major land use types. An overview of the Wala basin's land use is shown in Table 2.

Table 2. Land cover distribution (Hawamdeh et al., 2024)

Landcover	Area [ha]	%Area
Water	87.7	0.05
Forest-Mixed	80.2	0.05
Agricultural Land-Row Crops	17563.0	9.88
Residential-Medium Density	19419.2	10.92
Barren	116991.8	65.79
Range-Brush	23686.7	13.32
Sum	**177828.6**	**100**

Soil Map

The soil map used in this study was obtained from the Food and Agriculture Organization and is valuable for land evaluation (Bani Baker et al., 2022; Jones et al., 2012). Table 3 provides a summary of the soil types in the Wala catchment.

Table 3. Soil types in the Wala watershed (Nachtergaele et al., 2012)

Soil Code/Type	Hydrology Soil Group	Area [ha]	% Area
Af17-1-2a-2: Sandy_Clay_Loam	C	70674.8	39.74
Af32-2ab-3: Sandy_Clay_Loam	D	104539.1	58.79
Bc8-2b-7: Loam	C	2614.7	1.47
Sum		**177828.6**	**100**

Probable Maximum Precipitation (PMP) and Probable Maximum Flood (PMF)

Historical flood records, alongside meteorological and hydrological datasets, are vital for gauging the potential scale of the Probable Maximum Flood (PMF) (Lee & Yoo, 2023). This scenario is evaluated using the Hershfield formula, which is a statistical method through which the maximum amount of precipitation is estimated over a specific period of time.

Hydrologic Simulation

Watershed Modeling System (WMS, 2024) uses topographical information, soil properties, rainfall data, land use data, and certain hydrological characteristics specific to the study area. These inputs are essential for simulating flood drainage patterns arising from intense rainfall events (Minashkina et al., 2020). Typically, the hydrological modeling method integrates the SCS-CN method as part of its input, facilitating the calculation of surface run-off generation (Soulis, 2021). Two different routing techniques were used in the constructed hydrological model to faithfully simulate water flow in the system. By using volume-elevation curves and spillway discharge values unique to the WAD, this technique guarantees precise water flow modeling through the reservoir.

Hydraulic Simulation

The 2D-SWE constitutes a trio of partial differential equations to solve for three unknowns that are delineated across a 2D spatial domain as:

$$\frac{\partial h}{\partial t}+\frac{\partial q_X}{\partial X}+\frac{\partial q_Y}{\partial y}=i-f$$

where q_X, q_Y are the 2D components of the unit discharge, h is the water depth, i is the rainfall intensity, and f is the soil infiltration rate. The model was designed to analyze failure scenarios involving overtopping. Utilizing the Hershfield technique, the PMF was estimated.

Using the RAS Mapper tool of the HEC-RAS program, the dam's location is incorporated and connected to the two-dimensional flow area, as shown in Figure (2). The initial conditions for overtopping failure are summarized in Table 4.

Figure (4): Location of reservoir storage area, 2D flow area and dam

Dam Breach Parameters

It is important to identify the mechanisms of breach and the subsequent unsteady flow conditions. These breach mechanisms are determined through the establishment of a regression relationship between the breach parameters and the characteristics of the dam. To develop a procedure for estimating the potential dam breach mechanisms and behavior, as well as the consequences of the resulting flood wave, it is necessary to gather information about the dam's characteristics, such as its construction type, reservoir volume, height, and length. Assessing the potential consequences of a dam failure is crucial to the overall analysis of the breach mechanism (Psomiadis et al., 2021). The equations which will be used to estimate the breach parameters are: MacDonald and Langridge-Monopolis (1984), von Thun and Gillette (1990), Froehlich (2008b) and Xu and Zhang (2009) equations.

MacDonald and Langridge-Monopolis (1984) equation (MacDonald & Langridge-Monopolis, 1984).

$$Veroded = 0.0261\ (Vout\ \ hw)0.769$$
$$tf = 0.0179\ (Veroded)^{0.364}$$

where: *Veroded*: volume of material eroded from the dam embankment (cubic meters), *Vout*: volume of water discharged out the breach, *hw*: height of water above the breach bottom (meters) and *tf*: breach formation time (hours).

Von Thun and Gillette (1990) (Von Thun & Gillette, 1990b).

$$Bave = 2.5\ hw + Cb$$
$$tf = 0.02\ hw + 0.25$$

where: *Bave*: average value of the breach width (meters), *hw*: the height of water over the bottom of breach (meters) and C_b: coefficient depending on reservoir size, and Table 4 shows the value of C_b.

Table 4. C_b value for von Thun and Gillette equation

Reservoir Size (cubic meters)	C_b (meters)	Reservoir Size (acre-feet)	C_b (feet)
< 1.23^x10^6	6.1	< 1,000	20
$1.23^x10^6 - 6.17{*}10^6$	18.3	1,000 - 5,000	60
$6.17^x10^6 - 1.23{*}10^7$	42.7	5,000 - 10,000	140
> 1.23^x10^7	54.9	> 10,000	180

Froehlich (2008b) (Froehlich, 2008).

$$Bave = 0.27\ Ko\ Vw0.32\ h_b^{0.04}$$
$$tf = 63.2\sqrt{\frac{Vw}{gh_b^2}}$$

where: B_{ave}: average value of the breach width (meters), *Ko*: constant number = 1.3 for overtopping failures, V_w: volume for storage at the time of failure (cubic meters), h_b: height of breach (meters), *g*: gravitational acceleration (9.81 m^2/sec), t_f: breach formation time (hours).

Xu and Zhang (2009).

Xu and Zhang developed an equation to calculate the average breach width of dams as shown below:

$$\frac{B_{ave}}{h_b} = 0.787\ (\frac{h_d}{h_r})^{0.133} \times (\frac{V_w^{1/3}}{h_w})^{0.652} e^{B_3}$$

where, B_{ave} is the average breach width in meters, V_w is the storage volume at the time of failure in cubic meters, h_b is the breach height in meters, h_d is the dam height in meters, and h_r, set at 50 meters, is a reference height for comparing large and small dams, h_w represents the water depth over the bottom of the breach at the time of breach formation, and B_3 is a constant determined by the summation of b3, b4, and b5, which are coefficients dependent on dam properties.

The constant b3 varies based on dam type, with values of −0.041 for corewall dams, 0.0260 for concrete-faced dams, and −0.226 for homogeneous or zoned-fill dams. b4 reflects the failure mode, with values of 0.1490 for overtopping and −0.389 for seepage or piping. Finally, b5 represents the dam's erodibility, taking values of 0.2910 for high, −0.14 for medium, and −0.391 for low erodibility.

Xu and Zhang's research (Xu et al., 2009) does not directly provide estimates for side slopes. However, they developed a formula to calculate the breach top width, which, when combined with the average breach width, can be used to determine the corresponding side slopes. The equation for the breach top width is as follows:

$$\frac{B_t}{h_b} = 1.062\,(\frac{h_d}{h_r})^{0.092} \times (\frac{V_w^{1/3}}{h_w})^{0.508} e^{B_2}$$

where B_t is the breach top width in meters, B_2 is a constant dependent on b3+b4+b5, which are coefficients based on dam properties. The value of b3 is 0.06 for corewall dams, 0.088 for concrete-faced dams, and -0.089 for homogeneous/zoned-fill dams. The value of b4 is 0.299 for overtopping and -0.239 for seepage/piping. Lastly, b5 is 0.411 for high dam erodibility, -0.062 for medium dam erodibility and -0.289 for low dam erodibility.

Breach side slopes can be calculated using the following equation:

$$Z = \frac{B_t - B_{ave}}{h_b}$$

$$\frac{T_f}{T_r} = 0.304\,(\frac{h_d}{h_r})^{0.707} \times (\frac{V_w^{1/3}}{h_w})^{1.228} e^{B_5}$$

where: T_f is the breach formation time (hours), T_r is 1 hour (unit duration, B_5 is a constant dependent on b3+b4+b5 coefficient that is a function of dam properties. b3 is -0.327 for corewall dams, -0.674 for concrete-faced dams, and -0.189 for homogeneous/zoned-fill dams. b4 is -0.579 for overtopping and -0.611 for seepage/piping. b5 is -1.205 for high, -0.564 for medium, and 0.579 for low dam erodibility.

Define initial conditions for overtopping and piping failure. Table 5 summarizes the initial condition for each failure.

Table 5. Initial conditions for overtopping and piping failures (MWI, 2022)

Initial Condition	Piping	Overtopping
Top of dam	539	539
Pool elevation at failure	531	539
Breach bottom elevation	519	500
Reservoir volume at failure (thousands of m^3)	15625	22041
Crest width	9	9

A 2D unsteady hydraulic modeling using HEC-RAS simulation is developed. Firstly, a lateral inflow hydrograph is entered for the reservoir, with hydrograph data exported from WMS for Probable Maximum Flood (PMF) scenarios. The second boundary condition is set as normal depth for the 2D area. The initial flow is estimated based on the spillway's design capacity, as the dam breach is analyzed for the worst-case flood scenario. The initial water level is set as either the elevation of the maximum pool level or the crest of the dam.

Flood Hazard Mapping

The process of flood hazard mapping involves identifying areas vulnerable to floods in various circumstances by simulating river flow, storm water run-off, and the extent of inundation covered by water under different scenarios. located at different elevations from flood-prone areas. Five levels of risk hazards are identified from low hazard H1 to extremely high hazard H5 (Peker et al., 2024; Shatanawia et al.).

RESULTS AND DISCUSSION

A two-dimensional unsteady hydraulic model simulates the flood resulting from a dam break. The duration of the simulation was determined by looking at the dam's PMF hydrograph. The results were evaluated and displayed using RAS-Mapper, which made it possible to construct a number of flood inundation maps depending on parameters including depth, velocity, water surface elevation, arrival time, inundation boundary, and flood duration.

Estimation of PMP

The intended storm was calculated using the Hirschfield statistical approach, and its possible influence on flood mapping was assessed. The PMP for every station in the watershed is shown in Table 6.

Table 6. The PMP for different stations in Wala catchments (by the authors)

Station ID	Station	Location: Jordan Coordinates		Probable Maximum Precipitation (mm)
		Northing (m)	Easting (m)	
CD0003	El-Muwaqqar	521495	415576	72.4
CD0028	Muleih	496344	388163	109.3
CD0006	Wadi Wala Evap.St.	493026	383109	93.7
CD0018	Khanez-Zabeeb	482807	414942	62.3
CD0017	Um El-Risas	486291	397499	73.5
CD0015	Dhaba' Nursery	496676	410669	54.7
CD0007	Dhiban	486311	383999	114.0
CD0005	Jiza	508228	401358	69.0

PMF Hydrograph

The PMF flood hydrograph has a peak flow of 2,621 m^3/s as obtained from the PMF's routed hydrograph. This could lead to water levels rising above the dam crest. This elevated risk makes overtopping failure the most likely failure by significantly increasing the probability of its occurrence.

Dam Breach Flow Hydrograph

The overtopping and piping failure breach parameters are compiled in Table 7. Notably, these characteristics can be automatically calculated using HEC-RAS.

Table 7. Overtopping and piping failure breach parameter (by the authors)

Breach Parameter	Overtopping			Piping		
Method	Bottom breach width (m)	Side slope (H:1V)	Breach formation time (hrs)	Bottom breach width (m)	Side slope (H:1V)	Breach formation time (hrs)
MacDonald et al. (1984)	44	0.5	1.35	21	0.5	1.13
Froehlich (2008)	52	1	0.67	35	0.9	0.61
Von Thun and Gillette (1990)	133	0.5	1.03	113	0.5	0.87
Xu & Zhang	91	1.02	1.09	59	0.60	1.22

In the HEC-RAS framework, the breach flow hydrographs for overtopping and piping failures are shown in Figures (5) and (6), respectively. Using the Xu & Zhang equation, the results show that the highest breach flow for an overtopping collapse was 12435.48 m^3/s. Using the formulae from MacDonald et al. (1984), Froehlich (2008), and von Thun and Gillette (1990) (Al-Salahat et al., 2024; MacDonald, 1984; von Thun and Gillette, 1990a), in contrast, the highest breach flows were predicted to be 5962.15 m^3/s, 5146.99 m^3/s, and 9566.42 m^3/s, respectively. Using von Thun and Gillette, the maximal breach flow for the piping failure scenario was 5962.05 m^3/s. Using Froehlich (2008), the peak breach flood values for piping failure were 3331.04 m^3/s, 4205.83 m^3/s, and 4435.19 m^3/s, respectively.

Flood Inundation and Water Depth Map

The Wadi Wala urban area's possible flood damage is visually shown by the flood inundation map. In narrow sections of the wadi, the predicted water depths resulting from the dam failure are 42.7 m for overtopping failure and 28.9 m for piping failure. Figure (7) shows the water depth and inundation map for overtopping failure.

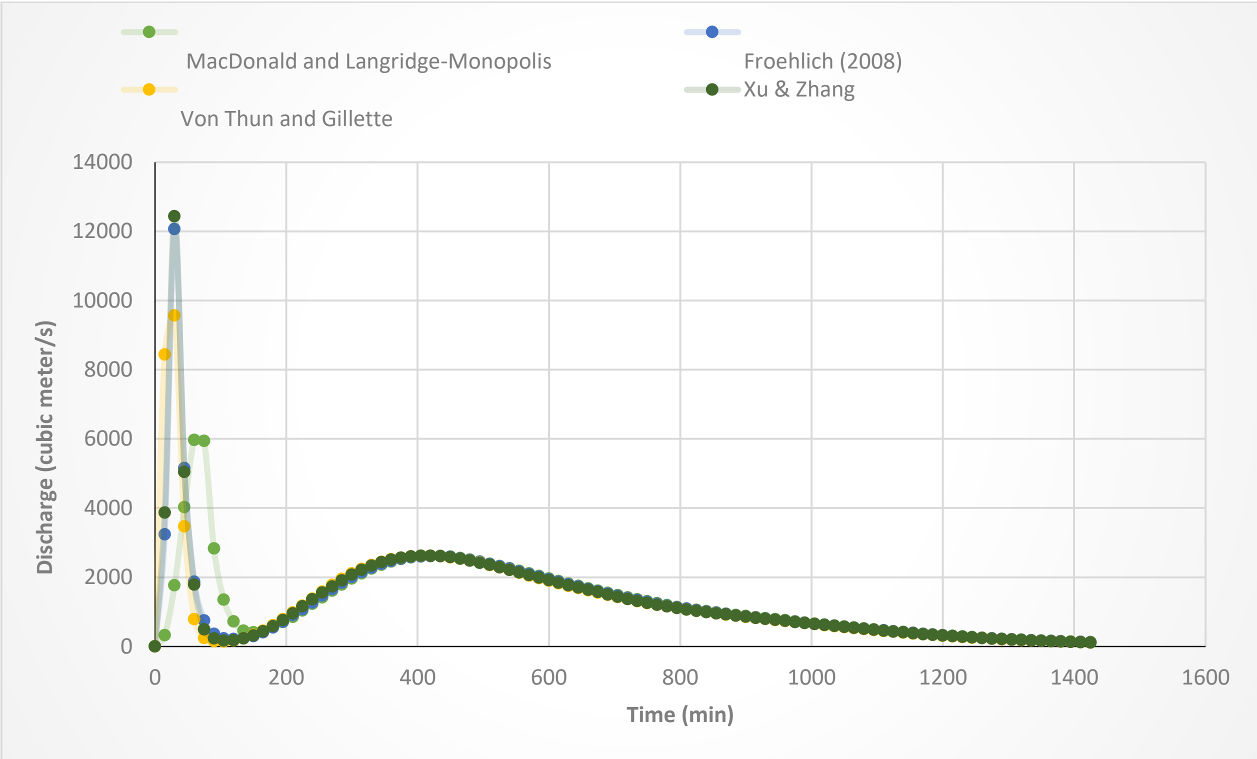

Figure (5): Breach flow hydrograph for overtopping failure in the downstream area of Wala dam

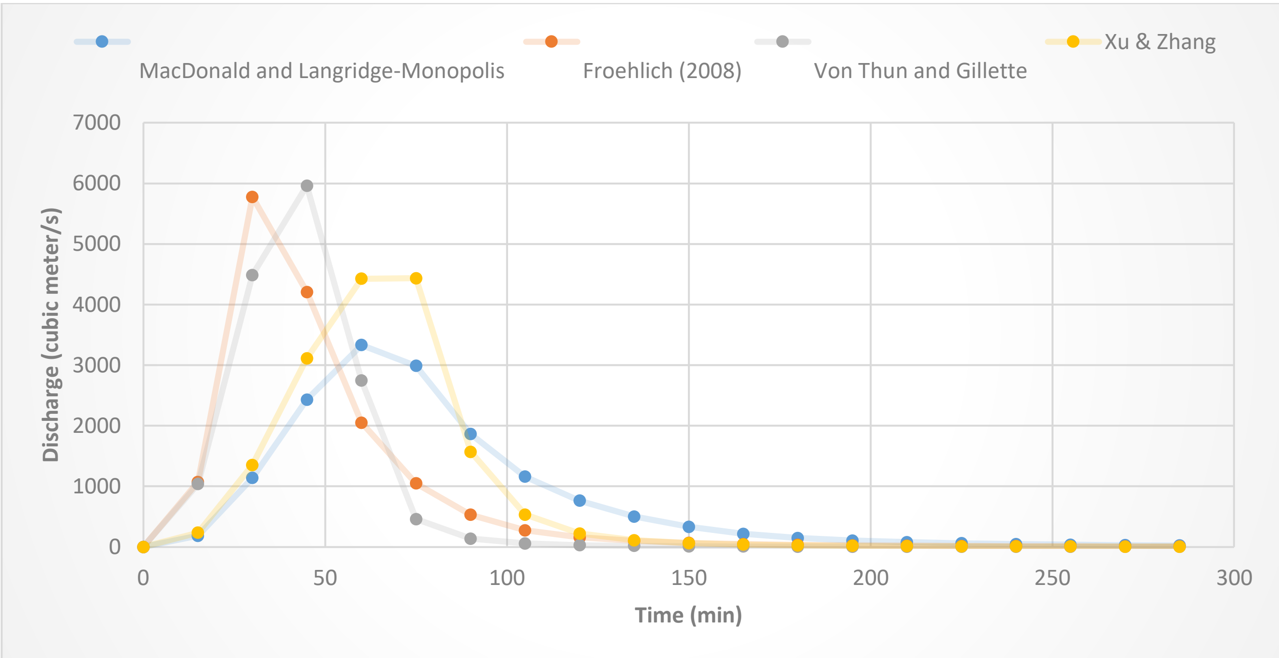

Figure (6): Breach flow hydrograph for piping failure in the downstream area of Wala dam

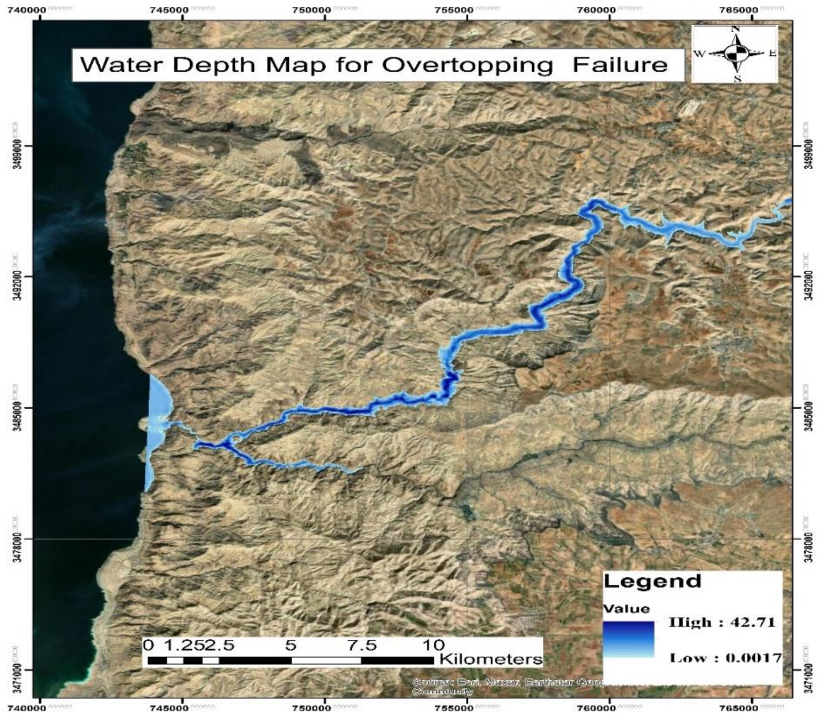

Figure (7): Water depth and flood inundation map for overtopping failure

Flood Hazard Maps

Flood hazards have been categorized based on water depth into five distinct levels, as shown in Figure (8). Five different levels of flood dangers have been identified based on the depth of water. The danger classification map for the overtopping failure scenario covers a larger area than the piping-failure scenario. Nearly 90% of the downstream regions are classified as extremely hazardous, denoted by H5 according to the hazard map. This represents a significant share of the downstream territories.

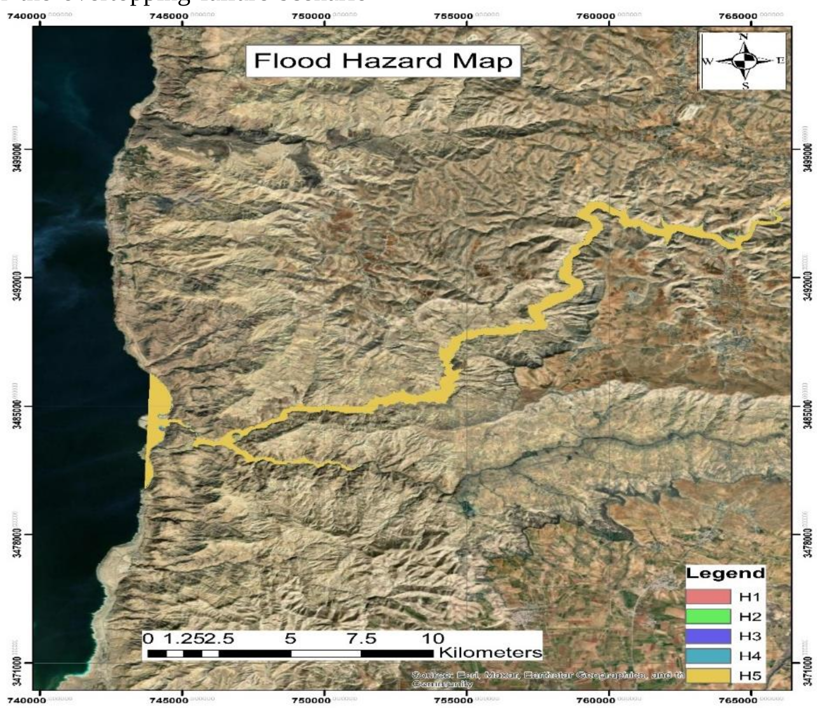

Figure (8): Flood hazard map for overtopping failure

Water Velocity Maps

The breach flow reached maximum velocities of 17.1 m/s for overtopping failure and 15.8 m/s for piping failure, respectively, as shown in Figure (9).

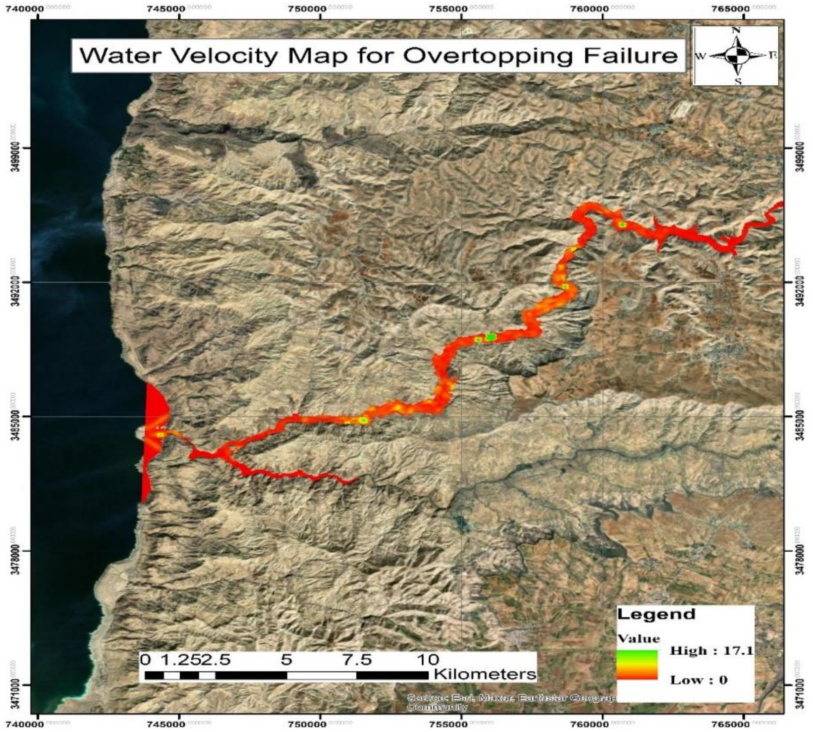

Figure (9): Velocity map for overtopping failure

The estimated arrival time of the flood wave to Wadi Wala was calculated for two failure scenarios: overtopping failure and piping failure. In the case of overtopping failure, the flood wave takes approximately 23 minutes to reach the first Dead Sea road.

CONCLUSIONS AND RECOMMENDATIONS

Two dam breach failures are investigated: overtopping failure and piping failure. The hydraulic model for 2-dimensional unsteady flow was utilized to direct the breach water downstream of the dam. In the overtopping and piping scenarios, the maximum peak flows were 12,435 m³/s and 5,962 m³/s, respectively. For places downstream of the dam, the data was used to create maps of inundation, flood hazard risk, duration, and velocity. Extreme hazard zones cover the majority of the flooded areas. In certain agricultural areas, the maximum water depth for an overtopping failure is roughly 43 meters, while it is approximately 8 meters close to the Dead Sea Road. Farm buildings, roads, bridges, the Dead Sea Road, and other significant public and private properties are among the sites that have flooded. Additionally, the maximum velocities for piping failure and overtopping failure are 15.8 m/s and 17.1 m/s, respectively. This study highlights how crucial effective emergency preparation is to reduce possible harm. Additionally, it provides helpful resources for calculating the flood risk linked to the two failure scenarios for the Wala Dam.

It is recommended to have early warning monitoring systems in place to find early indicators of dam failure. To guarantee that communities downstream receive timely warnings, this involves automated alarm systems, remote sensing technology, and routine inspections.

To make sure that everyone knows what to do in the case of dam break, it is necessary to create and update comprehensive emergency preparedness plans on a regular basis through drills and simulations involving local authorities and communities. This involves using community-based disaster risk reduction initiatives to strengthen the resilience of populations downstream.

In summary, this study provides valuable insights into the dynamics of dam breach floods and their effects on downstream regions. These findings could aid in developing plans and policies to minimize the risk of loss of life and property due to dam failure.

Conflict of Interests

The authors declare that there is no conflict of interests for publication of this manuscript. In addition, the ethical issues, including plagiarism, informed consent, data fabrication and/or falsification, double publication and/or submission have been completely observed by the authors.

Data Availability

The data that supports the findings of this study is available from the corresponding author, Dr. Radwan Al-Weshah, upon reasonable request.

Author Contributions

All authors contributed to the study's conception, data collection, analysis, modeling design and manuscript preparation.

Acknowledgements

This research was carried out during the sabbatical leave granted to the first author Radwan Al-Weshah from the University of Jordan during the academic year 2023/2024.

The first author acknowledges this support. The authors thank Al-Zaytoonah University of Jordan for partially funding this research. Furthermore, the authors are extremely thankful to the reviewers for their insightful comments.

REFERENCES

Alhasan, Z., Jandora, J., and Říha, J.J.A.U.A.e.S.M.B. (2015). "Study of dam break due to overtopping of four small dams in the Czech Republic". Acta Universitatis Agriculturae et Silviculturae Mendelianae Brunensis, 63 (3), 717-729.

Al-Salahat, M., Al-Weshah, R., and Al-Omari, S.J.S.W.R.M. (2024). "Dam break risk analysis and flood inundation mapping: A case study of Wadi Al-Arab dam". Sustainable Water Resources Management, 10 (2), 74.

Almawas, M., Azmi, M., and Baker, M.B.J.J.J.o.C.E. (2024). "Using statistical methods to analyze 32 years of rainfall data in Amman, Jordan". Jordan Journal of Civil Engineering, 18 (4).

Bani Baker, M., Abendeh, R., Sharo, A., and Hanna, A.J.C. (2022). "Stabilization of sandy soils by bentonite clay slurry at laboratory bench and pilot scales". Coatings, 12 (12), 1922.

Beza, M., Fikre, A., and Moshe, A.J.A.i.C.E. (2023). "Dam breach modeling and downstream flood inundation mapping using HEC-RAS model on the proposed Gumara dam, Ethiopia". Advances in Civil Engineering, 1 (2023), 8864328.

Caballero, F.J., Toledo, M.Á., Morán, R., and Peraita, J. (2022). "Performance of wedge-shaped block armoring for embankment dams and levees in a singular testing facility at quasi-prototype size".

Duressa, J.N., and Jubir, A.K.J.S.R. (2018). "Dam break analysis and inundation mapping: A case study of Fincha dam in Horro Guduru Wollega zone, Oromia region, Ethiopia". Science Research, 6 (2), 29-38.

Farhan, Y.J.J.o.G.I.S. (2017). "Morphometric assessment of Wadi Wala watershed, southern Jordan, using ASTER (DEM) and GIS". Journal of Geographic Information Systems, 9 (2), 158-190.

Froehlich, D.C.J.J.o.H.E. (2008). "Embankment dam breach parameters and their uncertainties". Journal of Hydraulic Engineering, 134 (12), 1708-1721.

Gray, R.E. (2017). "Geomechanics and water engineering in environmental management". Routledge.

Guimarães, R.N., Moreira, V.R., Cruz, J.R., Saliba, A.P., and Amaral, M.C.J.S.o.T.T.E. (2022). "History of tailings dam failure: Impacts on access to safe water and influence on the legislative framework". Science of the Total Environment, 852, 158536.

Hawamdeh, A., Tarawneh, A., Sharrab, Y., and Al-Fraihat, D. (2024). "Deep neural networks hydrologic and hydraulic modeling in flood hazard analysis".

Imbrogno, D.F. (2014). "Analysis of dam failures and development of a dam safety evaluation program". The Ohio State University.

Jiang, X., Wei, Y., Wu, L., Hu, K., Zhu, Z., Zou, Z., and Xiao, W.J.E.e.s. (2019). "Laboratory experiments on failure characteristics of non-cohesive sediment natural dam in progressive failure mode". Environmental Earth Sciences, 78, 1-14.

Jones, R., Le-Bas, C., Nachtergaele, F., Rossiter, D., van, J., Orshoven, R.S., van Velthuizen, H.J.J.S., Technical Report, E.C.J.R.C.I.f.E., and pdf, S.-I.L.A.o.h.m.i.h.t.a.J. (2012). "Updated common bio-physical criteria to define natural constraints for agriculture in Europe". RC Scientific and Technical Report, European Commission Joint Research Centre Institute for Environment and Sustainability-IES. Luxemburg. Available online at: http://members.iif.hu/tot3700/abstr/JVOJMTTT2012.pdf

Latrubesse, E.M., Park, E., Sieh, K., Dang, T., Lin, Y.N., and Yun, S.-H.J.G. (2020). "Dam failure and a catastrophic flood in the Mekong basin (Bolaven plateau), southern Laos, 2018". 362, 107221.

Lee, J., and Yoo, C.J.H.R. (2023). "Determination of Clark unit hydrograph parameters for estimating probable maximum flood". Hydrology Research, 54 (2), 245-264.

Liu, Z., Chen, Q., Li, X., Chen, C., Zhou, C., and Wang, C.J.N.H. (2023). "A review of research on the failure potential of landslide dams caused by overtopping and seepage". Natural Hazards, 116 (2), 1513-1538.

MacDonald, G.M.J.C.J.o.E. (1984). "New directions in the economic theory of agency". Canadian Journal of Economics, 415-440.

MacDonald, T.C., and Langridge-Monopolis, J.J.J.o.H.E. (1984). "Breaching charateristics of dam failures". Journal of Hydraulic Engineering, 110 (5), 567-586.

Minashkina, D., Happonen, A.J.I.J.o.S.C., and Management, I. (2020). "Systematic literature review and research gap issues on third party logistics operators selecting WMS for efficient operations for customers". International Journal of Supply Chain and Inventory Management, 3 (2), 142-166.

Nachtergaele, F., van Velthuizen, H., and Verelst, L.J.t.W.C.S.S.S.S.a.C.W. (2012). "Harmonized world soil database, version 1.2". Food and Agriculture Organization of the United Nations (FAO).

Peker, İ.B., Gülbaz, S., Demir, V., Orhan, O., and Beden, N.J.S. (2024). "Integration of HEC-RAS and HEC-HMS with GIS in flood modeling and flood hazard mapping". Sustainability, 16 (3), 1226.

Salamah, E., El-Hasan, T., and Abu-Jamah, M.J.E. (2023). "Dam safety in Jordan: Factors affecting dam safety, responsibilities and required actions". Engineering, 15 (9), 514-532.

Shatanawia, K., Al-Weshaha, R., Ta'anyc, R., Mohammadd, A.H., Kassaba, G., and Halalshehd, M. "Assessment and mapping of flash flood hazard and risk at Wadi Al-Yutum basin in Jordan: Integrating hydrological and hydraulic modeling techniques".

Solava, S., and Delatte, N. (2003). "Forensic engineering". In: Forensic Engineering, 178-189.

Soulis, K.X.J.W. (2021). "Soil conservation service curve number (SCS-CN) method: Current applications, remaining challenges, and future perspectives". Water, 192, MDPI.

Ta'any, R.A.J.I.J.o.A.R. (2011). "Impact of Wala Dam on groundwater enhancement of Wadi Wala catchment area in Jordan". Indian Journal of Agricultural Research, 45 (4), 255-265.

Tarawneh, Z.J.J.J.o.C.E. (2022). "The characteristics of the Wala dam monthly inflows and the relation to outflows". Jordan Journal of Civil Engineering, 16 (3).

Von Thun, J.L., and Gillette, D.R. (1990). "Guidance on breach parameters". US Department of the Interior, Bureau of Reclamation.

Von Thun, J.L., and Gillette, D.R.J.U.B.o.R. (1990b). "Guidance on breach parameters". Unpublished internal document.

Vozinaki, A.-E.K., Morianou, G.G., Alexakis, D.D., and Tsanis, I.K.J.H.S.J. (2017). "Comparing 1D and combined 1D/2D hydraulic simulations using high-resolution topographic data: A case study of the Koiliaris basin, Greece". Hydrological Sciences Journal, 62 (4), 642-656.

Xu, Y., Zhang, L.M.J.J.o.G., and Engineering, G. (2009). "Breaching parameters for earth and rockfill dams".

Yang, M., Cai, Q., Li, Z., and Yang, J.J.S.R. (2023). "Uncertainty analysis on flood routing of embankment dam breach due to overtopping failure". Scientific Reports. Journal of Geotechnical and Geoenvironmental Engineering, 13 (1), 20151.

Yilmaz, K., Darama, Y., Oruc, Y., and Melek, A.B.J.N.H. (2023). "Assessment of flood hazards due to overtopping and piping in Dalaman Akköprü dam, employing both shallow water flow and diffusive wave equations". Natural Hazards, 117 (1), 979-1003.

Zhang, J.-y., Fan, G., Li, H.-b., Zhou, J.-w., and Yang, X.-g.J.E.G. (2021). "Large-scale field model tests of landslide dam breaching". Engineering Geology, 293, 106322.